Journal Pre-proofs

Insights into the phenomenon of acquisition and accumulation of Fe^{3+} in *Hygrophila spinosa* through fluorimetry and fluorescence images

Ayndrila Ghosh, Saurodeep Mandal, Sujoy Das, Pallab Shaw, Ansuman Chattopadhyay, Prithidipa Sahoo

PII: S0040-4039(19)31319-X
DOI: https://doi.org/10.1016/j.tetlet.2019.151520
Reference: TETL 151520

To appear in: *Tetrahedron Letters*

Received Date: 6 November 2019
Revised Date: 9 December 2019
Accepted Date: 12 December 2019

Please cite this article as: Ghosh, A., Mandal, S., Das, S., Shaw, P., Chattopadhyay, A., Sahoo, P., Insights into the phenomenon of acquisition and accumulation of Fe^{3+} in *Hygrophila spinosa* through fluorimetry and fluorescence images, *Tetrahedron Letters* (2019), doi: https://doi.org/10.1016/j.tetlet.2019.151520

Graphical Abstract

To create your abstract, type over the instructions in the template box below.
Fonts or abstract dimensions should not be changed or altered.

Insights into the phenomenon of acquisition and accumulation of Fe^{3+} in *Hygrophila spinosa* through fluorimetry and fluorescence images

Ayndrila Ghosh[†][a], Saurodeep Mandal[†][a], Sujoy Das[a], Pallab Shaw[b], Ansuman Chattopadhyay[b] and Prithidipa Sahoo*[a]

[†]These authors contributed equally to this work.

Leave this area blank for abstract info.

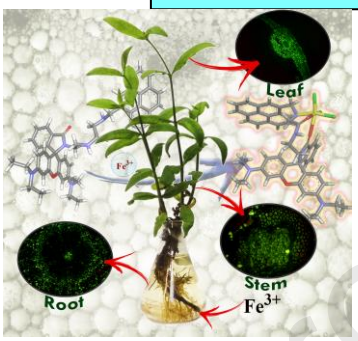

ELSEVIER

Tetrahedron Letters
journal homepage: www.elsevier.com

Insights into the phenomenon of acquisition and accumulation of Fe^{3+} in *Hygrophila spinosa* through fluorimetry and fluorescence images

Ayndrila Ghosh[†a], Saurodeep Mandal[†a], Sujoy Das[a], Pallab Shaw[b], Ansuman Chattopadhyay[b] and Prithidipa Sahoo*[a]

[a]*Department of Chemistry, Visva-Bharati, Santiniketan-731235, West Bengal, India.*
[b]*Department of Zoology, Visva-Bharati, Santiniketan-731235, West Bengal, India.*
[†] *These authors contributed equally to this work.*

ARTICLE INFO

Article history:
Received
Received in revised form
Accepted
Available online

Keywords:
Hygrophila
Iron accumulation
Chemosensor
Fluorescent Sensing
Estimation of Fe(III)

ABSTRACT

Rhodamine functionalized fluorescent probe **IP** has been synthesized to investigate the phenomenon of Fe^{3+} acquisition and accumulation in Hygrophila spinosa. H. spinosa is a tropical medicinal plant which is iron rich and consumed for the treatment of the patients suffering from anaemia. **IP** is capable of selectively binding Fe^{3+} by enhancing fluorescent intensity via "turn on" mechanism due to complex formation. Spectroscopic studies and microscopic tools helped in better understanding about the acquisition as well as the quantitative accumulation of Fe^{3+} in different parts of the plant.

1. Introduction

Hygrophila spinosa- a medicinal plant mostly found in tropical climate and the leaves of the plant are often used as a part of the daily cuisine especially in eastern India. Traditionally, the stem and leaves are being used for centuries to improve in haemoglobin level in blood to treat patients suffering from anaemia as it is Iron rich in nature. The plant also shows anti-inflammatory [1-3], antipyretic [4,5], hematopoietic[6], antioxidant[7-9], antibacterial[10,11] and anthelmintic [10] effects. Previous studies on different other plant systems indicate, acquisition of iron occurs via two major pathways:(i) by releasing H^+- ATPase from the root of the rhizosphere which extrudes H^+ ions to lower the pH and increasing the solubility of Fe^{3+}. Consequently an inducible ferric chelate reductase FRO2 reduces Fe^{3+} to Fe^{2+}.[12,13] The Fe^{2+} being transported by a major transporter IRT1 from root to other parts of the plants[14,15]; (ii) by secreting Phytosiderophores and the chelated Fe^{3+} then transported to different organisms of the plant.[16] Literature suggests that Iron mostly exists in the form of Fe^{2+} and Fe^{3+} in the soil. However, the intake process and method of accumulation of iron within the physiological system of *Hygrophila spinosa* has not been definitively established yet, whether this accumulation occurs in the form of Fe^{3+} or by transforming it into Fe^{2+}. The current knowledge on human metabolic processes indicates iron is easily absorbed in the form of Fe^{2+} and therefore, all the external iron supplements are found to exist in Fe^{2+} state. Fe^{2+} ions get absorbed in the duodenum cells and rapidly oxidized to Fe^{3+}. Then, the Ferric ions bind with intracellular carriers and transported to different cells and organs of the human body.[17] [1]

Ferric ions are incorporated in the catalytic site of many proteins and enzymes.[18-21] Formation of met-haemoglobin, which is incapable of binding oxygen, induced by the oxidation of haeme iron to ferric ion.[12] Increased accumulation of ferric ions in a living cell can generate reactive oxygen species (ROS) via the Fenton reaction[19], which can damage lipids, nucleic acids, and proteins. The cellular toxicity of ferric ions are connected to severe diseases like Alzheimer's, Huntington's, and Parkinson's disease, colorectal cancer.[22-25]

Our interest is to find out the quantitative accumulation of Fe^{3+} within *H. spinosa*. Several analytical methods such as colorimetry, UV-Vis spectrometry, atomic absorption and inductively coupled plasma mass spectrometry, flow injection analysis, column preconcentration, catalytic cathodic stripping voltammetry are commonly used for iron determination.[26-29] But fluorescent chemosensors become predominantly popular for their lion's share in the intrinsic features of a practical sensing system.[30-36] Hence, the present work relates to the designing of a

[1] ∗ Corresponding author. Prithidipa Sahoo, e-mail: prithidipa@hotmail.com

detection and estimation of Fe^{3+} in *H. spinosa*. Here we are introducing a rhodamine-pyrene conjugate fluorescence probe (**IP**) which has been applied to selectively determine and estimate the Fe^{3+} ions present in various parts of the *H. spinosa*. Though a large number of fluorescent probes have already been developed to detect Fe^{3+}, but most of them are not exclusively selective for Fe^{3+}. Probe IP is capable of detecting Fe^{3+} at very low concentration compared to others. Moreover, IP doesn't show any toxicity inside plant cells as well as tissues and hence it could be a potential dye to be used in living system. As the literature suggests, no previous work has been done in which qualitative accumulation of Fe^{3+} has been measured in living plant tissues to obtain the idea of acquisition and accumulation of inside plant cells (Comparison table SI).

Probe **IP** was synthesized through three simple steps starting from a very well-known fluorophore rhodamine and the structure of **IP** was deduced by ^1H and ^{13}C NMR spectral studies(Fig. S1& Fig.S2).

2. Experimental Section

2.1. Materials and Methods

Rhodamine B, ethylene diamine, bromoacetyl chloride, 1-pyrrenemethylamine, potassium carbonate, all the metal salts used for selectivity test were purchased from Sigma-Aldrich Pvt. Ltd. (India). All the materials were bought from commercial suppliers and were used without further purification. Standard procedures were obtained for solvent drying. Double distilled water was used throughout all experiments. ^1H and ^{13}C NMR spectra were recorded on a Bruker 400 MHz instrument. For NMR spectra and titration DMSO-d_6, D_2O were used as solvent using TMS as an internal standard. Chemical shifts are expressed in δ ppm units and ^1H–^1H and ^1H–C coupling constants in Hz. Fluorescence spectra were recorded on a PerkinElmer Model LS 55 spectrophotometer. UV spectra were recorded on a SHIMADZU UV-3101PC spectrophotometer. The following abbreviations are used to describe spin multiplicities in ^1H NMR spectra: s = singlet; d = doublet; t = triplet; m = multiplet.

2.2. Synthesis procedure.

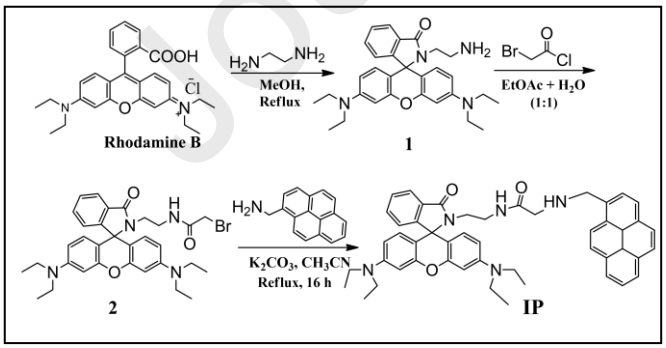

Scheme 1: Synthesis procedure of probe **IP**

2.2.1. Synthesis of 1

ne (20 mL). Ethylene diamine (5 mL, excess) was added drop-wise to the solution and refluxed overnight (15 h) until the solution loses its red color. The solvent was removed by evaporation. Water (20 mL) was added to the resultant and extracted with CH_2Cl_2 (20 mL × 2). The combined organic phase was washed twice with water and dried over Na_2SO_4. The solvent was removed by evaporation and dried in vacuum, affording a pale-pink solid of 1(3.80 g, yield, 79%).

2.2.2. Synthesis of 2

Compound 1 (1.5 g, 3 mmol) mixed with K_2CO_3 (4.27 g,10 mmol) is suspended into a mixture of ethyl acetate (25 mL) and water (25 mL) and stirred for 30 minutes. Then, bromoacetyl chloride (1.22g, 2.5 mmol) in ethyl acetate (5 mL) is added dropwise into the solution. After 4 h stirring at room temperature, the organic layer is isolated and dried by $MgSO_4$. The ethyl acetate solvent is removed by rotary evaporation to give the crude product that is purified by column chromatography (silica, 220–400 mesh, EtOAc/MeOH = 10:1 v/v). The product is isolated as a pale-pink powder 2 (1.26 g, 84%). Synthesis of intermediate 1 and 2 has been performed by following previously published protocols.[37]

2.2.1. Synthesis of IP

To a solution of anhydrous K_2CO_3 (2.5g, 18 mmol) in dry acetone was added 1-pyrrenemethylamine (0.55 g, 2.0 mmol). The mixture was stirred for 45 minutes. Then compound 2 (1.26 g, 2.0 mmol) was added to the solution and refluxed for 24 h (Scheme 1). Acetone was dried and the mixture was treated with brine (3×20mL). The organic layer was extracted with CH_2Cl_2 (3×50 mL), and the combined organic layer was washed with 5% aqueous HCl (50 mL), 10% aqueous Na_2CO_3 (50 mL) and finally with water and then was dried over anhydrous $MgSO_4$. After removal of solvents, the residue was chromatographed on silica gel (220–400 mesh) with chloroform/ethyl acetate=5:2 v/v as eluent to give 0.98 g (60%) of IP as a pink solid. ^1H NMR (DMSO-d_6, 400 MHz): δ (ppm) 8.39-8.37 (d, J = 9.2Hz, 1H), 8.31 (s, 1H), 8.26-8.22 (t, J = 16.4 Hz, 2H), 8.18-8.16 (d, J = 7.6 Hz, 1H), 8.12-8.09 (t, J = 9.2 Hz, 2H), 8.07-8.02 (m, J = 19.2 Hz, 2H), 7.80-7.78 (m, J = 8.4 Hz, 1H), 7.68-7.65 (t, J = 11.2 Hz, 1H), 7.48-7.46 (m, J = 8.8 Hz, 2H), 6.96-6.94 (m, J = 8.4 Hz, 1H), 6.35-6.34 (d, J = 2.4 Hz, 2H), 6.29 (s, 1H), 6.27 (s, 1H), 6.21-6.20 (d, J = 2.4 Hz, 1H), 6.19-6.18 (d, J = 2.4 Hz, 1H), 4.33 (s, 2H), 3.29-3.21 (m, J = 29.6 Hz, 8H), 3.14-3.12 (d, J = 9.6 Hz, 4H), 2.87-2.82 (m, J = 19.2 Hz, 2H), 1.23-1.20 (d, J = 8.0 Hz, 1H), 1.03-0.99 (t, J = 13.6 Hz, 12H). ^{13}C-NMR (DMSO-d_6, 400 MHz): δ(ppm) 170.86, 167.51, 153.63, 152.51, 148.31, 134.05, 132.69, 130.76, 130.29, 130.02, 129.87, 128.44, 128.15, 127.36, 127.15, 126.90, 126.78, 126.08, 125.01, 124.94, 124.59, 124.00, 123.96, 123.52, 123.48, 122.33, 108.01, 104.78, 97.24, 79.15, 64.02, 51.66, 50.33, 43.58, 40.14, 39.93, 39.72, 39.51, 39.30, 39.10, 38.89, 36.93, 20.72, 12.33. Anal.Calcd.for $C_{49}H_{49}N_5O_3$: C,

77.6 ns, 9.19; O, 6.30.

2.3. Computational calculations

Ground state optimizations of the structures were performed using Density functinal theory (DFT) for probe and the probe analyte complex i.e. **IP** and **IP**-Fe^{3+} complex have been studied using hybridexchange-correlation functionalB3LYP (Becke, three-parameter, Lee-Yang-Parr) and 6-31G**/LANL2DZ basis set implemented at Gaussian 09 program[26]. From the optimized structures of the **IP**-Fe^{3+} complex gives insight into the mode of binding of iron ion with the probe. CPCM (conductor-like Polarizable continuum model) solvent model has been used for H_2O medium to incorporate solvent effect in the computational calculations.

2.4. Fluorescence imaging

Two sets (**A** and **B**) of *H. Spinosa* saplings have been taken for the experiment. Where **A** has been submerged in H_2O designated as control (**C**). **B** has been treated with 1 mM $FeCl_3$ solution designated as treated (**T**). Two sets were kept for 25days**.** Dissections of all the parts (Root, stem and leaf) of both the matured plants were taken for fluorescence imaging. The samples after treating with **IP** solution for 1 hr, were observed with 10x magnification using FITC filter (519 nm) with excitation wavelength 490 nm under a fluorescence microscope (Dewinter, Italy) and the photographs were acquired through Biowizard image analysis software, Dewinter Optical Inc.

2.5.Quantitative estimation of Fe^{3+}

From the treated plant used for imaging, 2 g of root, stem and leaves have been taken and aqueous extracts were prepared by grinding. Double distilled H_2O has been used for extract preparation. The extracts were filtered through Whatman 41 filter paper, and then centrifuged at 6800 rpm at 25^oC for 8 minutes to eliminate unwanted particles. Using fluorescence spectroscopic data the concentration of Fe^{3+} present in plant cells has been estimated.

3. Results and discussion

3.1. UV-vis and fluorescence spectral behavior of IP with Fe^{3+}

Absorbance and fluorescence titrations were carried out in DMSO/H_2O (1:8, v/v), pH 7.0 (10 mM phosphate buffer) to investigate the interaction between probe **IP** and Fe^{3+} ion. In presence of Fe^{3+} , **IP** gives rapid responses with an absorption at 558 nm (Fig. 1a) along with the formation of two sharp isosbestic points at 330 nm and 344 nm. The molar extinction coefficient has been calculated from UV-absorption experiment. Considering λ_{max} at 342 nm ,ε was found to be 292600 M^{-1} cm^{-1} (see SI, UV-vis spectral studies). In fluorescence titration spectra about 18 fold enhancement in intensity at 580 nm (λ_{ex} = 490 nm) has been observed after the incremental addition of Fe^{3+} solution (Fig. 1b) whereas no change in intensity was found for other phosphates, amino acids and vitamin (Fig. S7) . The non-linear fitting analysis determined the association constant in the order of 25.5×10^4 M^{-1} for IP-Fe^{3+}complex (Fig. S3).The detection limit of probe **IP** was found to be 82 nM for Fe^{3+} (Fig. S4). The binding stoichiometry of probe **IP** and Fe^{3+} (Fig. S5) was evaluated 1:1 by Job's plot. Plot of fluorescence intensity as a function of time confirms that maximum of 20 minutes are required to complete this host-guest complexation (Fig. S6). pH titration of probe **IP** with Fe^{3+} revealed that the probe **IP** started to open the closed spirolactum ring at pH 6 and pink coloration is observed below pH 6. But surprisingly after complexation with Fe^{3+} the deep pink color persists even upto pH 8 (Fig. S8).

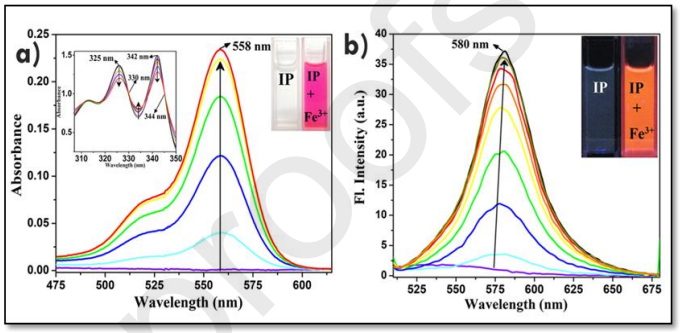

Figure 1.(a) UV-vis absorption spectra of **IP** (1 μM) in DMSO-water (1:8, v/v), 10 mM phosphate buffer (pH 7.0), upon addition of 1.5 equiv. Fe^{3+} solution. (Inset) Absorption spectra in the range of wavelength 310-350nm (b) Fluorescence emission spectra of **IP** (1 μM) in after addition of 1.5 equiv. of Fe^{3+} in DMSO-water (1:8, v/v), pH 7.0 (10 mM phosphate buffer) (λ_{ex} = 490 nm).

3.2. Selectivity of IP

The colorimetric observation illustrates that the addition of Fe^{3+} to the **IP** turned the colorless clear solution into dark pink while the addition of the other metal cations- Al^{3+}, As^{3+}, Fe^{2+}, Cu^{2+}, Cu^{+}, Zn^{2+}, Cd^{2+}, Pb^{2+}, Hg^{2+} and Ag^{+} to **IP** did not show any color change. When the similar experiment has been performed under UV lamp, it was observed that the complex showed a strong orange-red fluorescence but the presence of other metal cations in **IP** could not make any change to its inherent non-fluorescence (Fig. S9).

3.3. NMR experiments

NMR titration studies have been performed to elucidate the interactions of **IP** with Fe^{3+}. In ^1H NMR titration, upon sequential addition of 1 equiv. Fe^{3+} solution, the pyrene protons of **IP** shifted downfield gradually and the amide proton peak vanished. All the peaks became broader at the end of the titration (Fig.S10). This phenomenon is due to change in electron distribution between two fluorophores of probe **IP**. Also, the observation of the downfield shifting of spiro cycle carbon peak from 69 ppm to 150 ppm and disappearance of one of the carbonyl carbon peak at 170 ppm in ^{13}C NMR titration spectra just specifies a strong interaction between probe **IP** and its analyte Fe^{3+} ion (Fig. S11).

3.4. DFT calculations

The energy optimized structures of **IP** and **IP**-Fe^{3+} complex depict the mode of binding of $FeCl_3$ with probe **IP** (Fig. S12).

another carbonyl oxygen from the linker chain and nitrogen atom adjacent to pyrene moiety have satisfied three coordination sites of $Fe^{3+}$and other three sites of Fe^{3+} have been coordinated with chlorine atoms- these rise an octahedral geometry for **IP**-Fe^{3+} complex (Fig. 2).

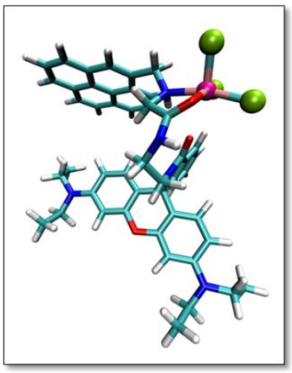

Figure 2. DFT optimized structure of **IP**-Fe^{3+} complex.

The total electron density has been calculated and mapped with ESP for **IP** and **IP**-Fe^{3+} complex. Figure 3(a) indicates that the electron density is much higher in oxygen atoms of the linker chain and partially higher in the amine nitrogen compare to that of pyrene moiety. Possibly electronic transition occurs from the electron donating centres (O,N) to Fe^{3+} to form a stable **IP**-Fe^{3+} complex (Fig. 3(b)).

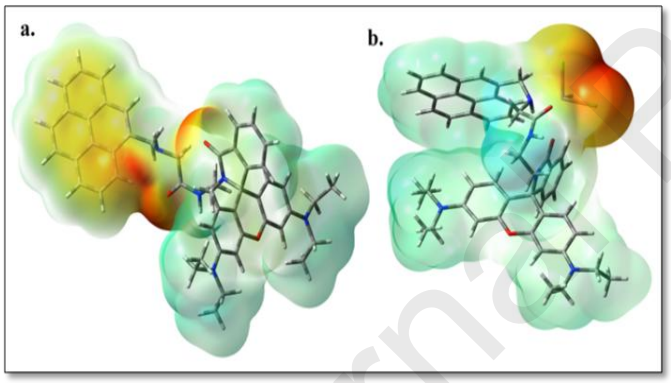

Figure 3.The total electron density (iso value=0.0004, -0.131e0-0.131e0) mapped with ESP for (a) **IP** and (b) **IP**-Fe^{3+}complex

Further NBO (Natural Bond Orbitals) analysis has been carried out to obtain a vivid picture about the binding phenomenon. Estimation of donor-acceptor (bond-antibond) interactions in the NBO basis has been done through second-order perturbative calculations. This analysis has been executed by examining all possible interactions between donor Lewis-type NBOs and acceptor non-Lewis NBOs. The hyperconjugative interaction energy was deduced from the second-order perturbation approach.[35]

The most important interactions between Lewis and non-Lewis orbitals with lone pairs are the second order perturbation energy values E(2). Parenthesized label numbers in Fig S13 , Table S3 and S4 show the number of bond pair and lone pair orbitals at each center. From the hyperconjugative interaction energy major interactions has been identified. In all the cases found to be participating as acceptor orbitals where as the bond pair orbitals of both the corbonyl groups, N-Hand C-N act as donor orbitals (Table S5). Thus these theoretical calculations evident the stabilization of **IP**-Fe^{3+}complex through E(2) values deduced for various molecular interactions.

3.6. Plausible mechanism and explanation

All the above experimental and theoretical findings firmly correlate the electronic properties of **IP**-Fe^{3+} complex. In UV-vis titration spectra, hike in absorption at the wavelength 558 nm indicates spirolactum ring opening of rhodamine moiety after the interaction between probe **IP** and Fe^{3+}. This ring opening is responsible for the strong coloration and fluorescence of **IP**-Fe^{3+} complex. Moreover, the presence of two distinct isosbestic points at 330 nm and 344 nm evident the formation of **IP**-Fe^{3+} complex and electron flow from pyrene moiety to electron deficit rhodamine part. The above interactions have also been established from the downfield shift of pyrene proton peaks in ^{1}H NMR titration.

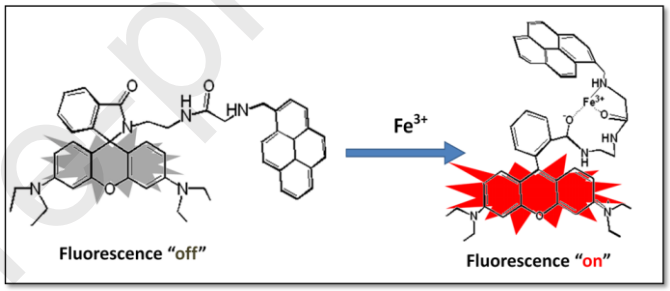

Scheme 2: Proposed binding mechanism of **IP** on addition of Fe^{3+}.

Furthermore, the disappearance of amide proton peak from ^{1}H-NMR spectra and spirolactum carbonyl carbon peak from ^{13}C-NMR spectra approve the non-covalent interaction of Fe^{3+} ion with them. Hence, the plausible binding approach of **IP** with Fe^{3+} has been shown in Scheme 2.

3.7. Fluorescence microscopic imaging of different parts of H. spinosa

Two healthy *H. spinosa* saplings were chosen and treated differently for imaging (Fig. S14 & Fig. 4).Root, stem and leaves from both the plants were dissected and observed under fluorescence microscope.

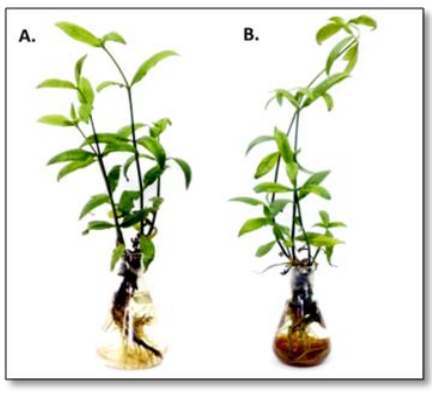

Figure 4. Matured *Hygrophila spinosa* a) in H2O, b) treated with 1 mM Fe3+ solution.

phenomena of accumulation of Iron(III) can be observed and it can be compared with the control plant (Fig. 5).

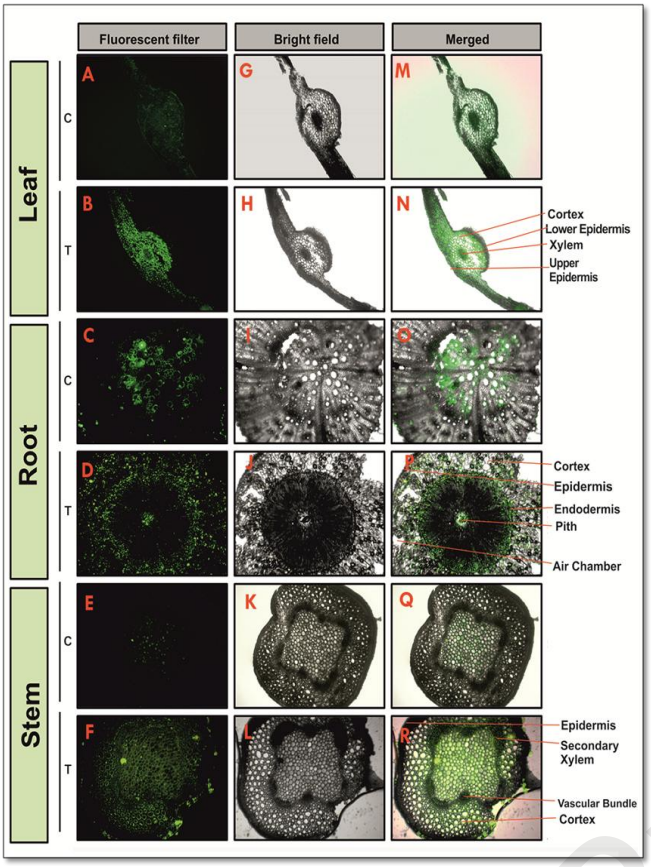

Figure 5. Fluorescence microscopic images of dissections of root, stem and leaf of *Hygrophila spinosa* plant (C= control , T= Treated with 1 mmolar Fe^{3+} solution) (A-F) are the fluorescent images, (G-L) are the corresponding brightfield images, and (M-R)are the corresponding overlay images.

In root, accumulation has been observed in endodermis

region, cortex and in pith. Where as in the dissection of the treated stem reveals that the accumulation of Fe^{3+} occurred mainly in secondary xylem, cortex, vascular bundle regions. In case of leaf, the accumulation was in xylem, phloem and cortex region. The above images describe that Fe^{3+} accumulation in leaf and stem is substantially high rather than root.

3.8.Quantitative estimation of Fe^{3+} in plant extracts

Estimation of Fe^{3+} in the treated plant extracts (root, stem and leaf) using fluorescence titration plot has been measured (Scheme 3).While plotting the data in the standard fluorescence titration curve, concentration of Fe^{3+} in 2ml of extract has been found out to be 0.35 µM and 0.74 µM for stem and leaf, respectively (Fig. 6).

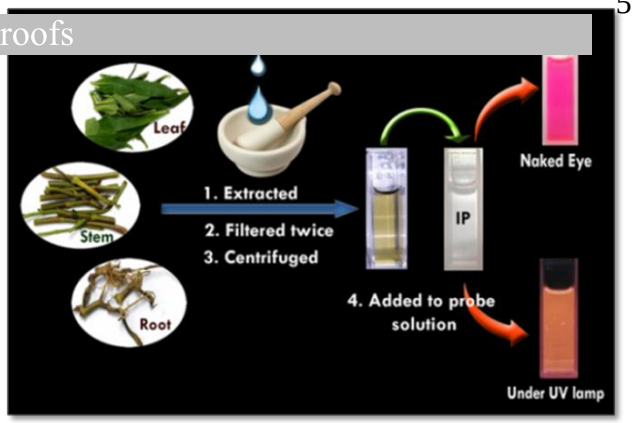

Scheme 3: Preparation of plant extracts

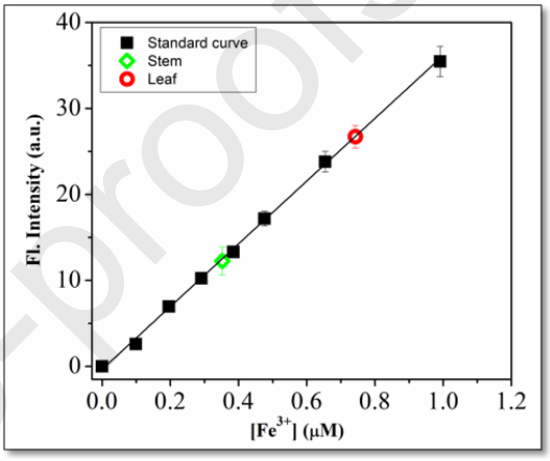

Figure 6. Estimation of Fe3+ ion in treated sapling of *Hygrophila spinosa* plant extracts. Standard deviations are given by error bars where, n=3.

To validate this experiment, Fe^{3+} has been added externally to the extract and for each sample almost 90% of fluorescence recovery has been found (Table S6).

4. Conclusion

Probe **IP** has been successfully synthesized, characterized and applied as a potential chemosensor for selective detection of Fe^{3+} ion in aqueous medium. Fe^{3+} interacts with the probe **IP** through three binding sites i.e. two carbonyl oxygen and one amine nitrogen present in **IP**. During stronger interaction the spirolactam ring of the rhodamine gets opened up and the electrons start flowing from pyrene to electron deficient rhodamine moiety. Spirolactum ring opening is responsible for the fluorescence "turn on" response of **IP** in presence of Fe^{3+} and the electron flow helps in the formation of stable **IP**-Fe^{3+} complex. All these phenomena has been well established by different spectrometric experiments along with theoretical calculations. The efficacy of **IP** has been employed to investigate the visualization as well as accumulation of Fe^{3+} ions in various parts of *Hygrophila spinosa* through fluorimetry even at nanomolar concentration. Fluorescence microscopic imaging studies suggests that accumulation of Fe^{3+} is more in leaf and stem compared to root. In future we are in progress to investigate

the , M.

plant system and storage of iron in such iron containing plants.

5. Acknowledgements

PS acknowledges CSIR, India for awarding her the start-up grant [Project file no. 02(0384)/19/EMR-II dated 20/05/2019]. AG and SD are sincerely thankful to UGC and CSIR, India respectively for the research fellowship. AG and SM also thank Kazi Tawsif Ahmed, Dept. of Botany, Visva-Bharati for his sincere help.

6. Notes

AUTHOR INFORMATION
Corresponding Author* E-mail: prithidipa@hotmail.com (P.S.).
ORCID Prithidipa Sahoo: 0000-0001-8493-7068
Ayndrila Ghosh: 0000-0003-1779-3863
Saurodeep Mandal : 0000-0003-0515-2209
Sujoy Das: 0000-0003-3921-0999

7. References

[1] Patra, A.; Jha, S.; Murthy, P. N.; D, A. V.; Chattopadhyay, P.; Panigrahi, G.; Roy, D. *Trop. J. Pharm. Res.* **2009**, *8(2)* (April), 133–137.
[2] Borgi, W.; Ghedira, K.; Chouchane, N. *Fitoterapia* **2007**, *78* (0269), 16–19. https://doi.org/10.1016/j.fitote.2006.09.010.
[3] Lipschitz, L.W. Activity on urinary tract. (Eds Vogel,G.H.; Vogel, H.W.) Drug Discovery and Evaluation. New York: Verlag Berlin Heidelberg Springer: **1997**. pp. 390-417
[4] Ahmed, N.; Hussain, S.; Ansari, Z. H. *Int. J. Heal. Res.* **2009**, *2*, 57–64
[5] Vijayakumar, M.; Govindarajan, R.; Rao, G. M. M.; Rao, C. V; Shirwaikar, A.; Mehrotra, S.; Pushpangadan, P. *J. Ethnopharmacol.* **2006**, *104*, 356–361. https://doi.org/10.1016/j.jep.2005.09.030.
[6] Pawar, R. S.; Jain, A. P.; Kashaw, S. K.; Singhai, A.K. *Indian J Pharm Sci.* **2006**, *3*, 337-40.
[7] Usha, K.; Kasturi, G. M.; Hemalatha, P. *Indian J. Clin. Biochem.* **2007**, *22* (2), 132–135. https://doi.org/10.1007/BF02913331.
[8] Malik, C. P.; Singh, M. B. Plant enzymology and histoenzymology. New Delhi: Kalyani Publishers: **1980**. p. 286.
[9] Shandrel, S. H. Method in food analysis. New York: Academic Press; (1970). p. 709.
[10] Römheld, V. Different Strategies for Iron Acquisition in Higher Plante. *Physiol. Plant.* **1987**, *70* (Strategy I), 231–234..
[11] Robinson, N. J.; Procter, C. M.; Connolly, E. L.; Guerinot, M. Lou. *Nature* **1999**, *397* (February), 4–7. https://doi.org/10.1038/17800.
[12] Eide, D.; Broderius, M.; Fettt, J.; Guerinott, M. Lou. *Proc. Natl. Acad. Sci. U. S. A.* **1996**, *93* (May), 5624–5628. https://doi.org/10.1073/pnas.93.11.5624.
[13] Henriques, R.; Klein, M.; Martinoia, E.; Feller, U.; Schell, J.; Pais, M. S.; Koncz, C. *Plant Mol. Biol.* **2002**, *50*, 587–597. https://doi.org/10.1023/A:1019942200164..
[14] Curie, C.; Panaviene, Z.; Loulergue, C.; Dellaporta, S. L.; Briat, J.; Walker, E. L.; Montpellier, Â. E. *Nature* **2001**, *409* (January), 346–349. https://doi.org/10.1038/35053080.
[15] Brugnara, C. *Clin. Chem.* **2003**, *49* (10), 1573–1578.
[16] Aisen, P.; Wessling-Resnick, M.; Leibold, E. A. *Curr. Opin. Chem. Biol.* **1999**, *3*, 200–206. https://doi.org/10.1016/S1367-5931(99)80033-7.
[17] Eisenstein, R. S. *Annu. Rev. Nutr.* **2000**, *20*,627-662.
[18] Rouault,T. A. *Nat. Chem. Biol.* **2006**, *2*, 406-414.
[19] Chai, M.; Li, M.; Zhang, D.; Wang, C. C.; Ye, Y.; Zhao,Y. *J. Lumin.* **2013**, *28*, 557-561.
A. *Metallomics.* **2011**, *3*, 267-270.
[21] Pithadia, A. S.; Lim, M. H. *Curr. Opin. Chem. Biol.* **2012**, *16*, 67-73.
[22] Zheng, H.; Weiner, L. M.; Bar-Am, O.; Epsztejn, S.; Cabantchik, Z. I.; Warshawsky, A.; Youdim, M. B. H.; Fridkin, M. Design, *Bioorganic Med. Chem.* **2005**, *13* (3), 773–783. https://doi.org/10.1016/j.bmc.2004.10.037.
[23] Glendening, E. D.; Badenhoop, J.K.; Reed, A. E.; Carpenter, J.E.; Bohmann, J. A.; Morales, C. M.; Weinhold, F. NBO 5.0, Theoretical Chemistry Institute, University of Wisconsin, Madison, **2001**.
[24] Kshirsagar, A. D.; Ingale, K. G.; Vyawahare, N. S.; Thorve, V. S. *Pharmacogn Rev.* **2010**, *4* (8), 167–171. https://doi.org/10.4103/0973-7847.70912.
[25] Micronutrient Information Center, Linus Pauling Institute, Oregon State University, Corvallis, Oregon. April 2016. Retrieved 6 March (2018).
[26] Chen, Y.T.; Jiang, J. *Org. Biomol. Chem.* **2012**, *10*, 4782.
[27] Pandey, R.; Gupta, R. K.; Shahid, M.; Maiti, B.; Misra, A.; Pandey, D. S. *Inorg. Chem.* **2012**, *51*, 298.
[28] Goswami, S.; Chakrabarty, R. *Eur. J. Org. Chem.* **2010**, *20*, 3791.
[29] Ratha, J.; Majumdar, K. A.; Mandal, S. K.; Bera, R.; Sarkar, C.; Saha, B.; Mandal, C.; Saha, K. D.; Bhadra, R. *Mol. Cell. Biochem.* **2006**, *290*, 113.
[30] Das, S.; Mukherjee, U.; Pal, S.; Maitra, S.; Sahoo, P. *Org. Biomol. Chem.* **2019**, 17, 5230-5233.
[31] Ghosh, A.; Das, S.; Kundu, S.; Maiti, P. K.; Sahoo, P. *Sensors and Actuators B: Chemical*. **2018**, *266*, 80–85.
[32] Das, S.; Rissanen, K.; Sahoo, P. *ACS Omega*. **2019**, *4*, 5270−5274.
[33] Sarkar, H. S.; Das, S.; Uddin, M. R.; Mandal, S.; Sahoo, P. *Asian J. Org. Chem*. **2017**, *6*, 71.
[34] Ghosh, A.; Das, S.; Mandal, S.; Sahoo, P. *New J. Chem.* **2019**, https://doi.org/10.1039/C9NJ03327K.
[35] Tang, A.; Chen, Z.; Deng, D.; Liu, G.; Tu, Y.; Pu, S. *RSC Adv.* **2019**, *9* (21), 11865–11869. https://doi.org/10.1039/c9ra02119a.
[36] Tang, A.; Yin, Y.; Chen, Z.; Fan, C.; Liu, G.; Pu, S. A *Tetrahedron* **2019**, *75* (36), 130489. https://doi.org/10.1016/j.tet.2019.130489.
[37] Das, S.; Sarkar, H. S.; Uddin, M. R.; Mandal, S.; Sahoo, P. *Sensors Actuators, B Chem.* **2018**, *259*, 332–338. https://doi.org/10.1016/j.snb.2017.12.040.
[38] Gaussian 09, Revision A.02, M. J. Frisch, G. W. Trucks, H. B. Schlegel, G. E. Scuseria, M. A. Robb, J. R. Cheeseman, G. Scalmani, V. Barone, G. A. Petersson, H. Nakatsuji, X. Li, M. Caricato, A. Marenich, J. Bloino, B. G. Janesko, R. Gomperts, B. Mennucci, H. P. Hratchian, J. V. Ortiz, A. F. Izmaylov, J. L. Sonnenberg, D. Williams-Young, F. Ding, F. Lipparini, F. Egidi, J. Goings, B. Peng, A. Petrone, T. Henderson, D. Ranasinghe, V. G. Zakrzewski, J. Gao, N. Rega, G. Zheng, W. Liang, M. Hada, M. Ehara, K. Toyota, R. Fukuda, J. Hasegawa, M. Ishida, T. Nakajima, Y. Honda, O. Kitao, H. Nakai, T. Vreven, K. Throssell, J. A. Montgomery, Jr., J. E. Peralta, F. Ogliaro, M. Bearpark, J. J. Heyd, E. Brothers, K. N. Kudin, V. N. Staroverov, T. Keith, R. Kobayashi, J. Normand, K. Raghavachari, A. Rendell, J. C. Burant, S. S. Iyengar, J. Tomasi, M. Cossi, J. M. Millam, M. Klene, C. Adamo, R. Cammi, J. W. Ochterski, R. L. Martin, K. Morokuma, O. Farkas, J. B. Foresman, D. J. Fox, Gaussian, Inc., Wallingford CT, (2016).

Res

- Rhodamine pyrene conjugate (**IP)** has been employed for selective estimation of Fe^{3+}.
- Investigation of accumulation of Fe^{3+} in *Hygrophila spinosa* by chemosensing method.
- Visualization of Fe^{3+} in different parts of *H. spinosa* through fluorescence microscopy.
- Spectroscopic and theoretical analysis were done to establish **IP**-Fe^{3+} interaction.